Study of Mechanical Properties of Nano-Structured Maraging Stainless Steel (C300)

Venkatesh Naik Nenavath[1] Bala Narsaiah. T[2] Shashi Kumar. A[3]
[1,2]JNTUA College of Engineering, Anantapuramu, Andhra Pradesh, India [3]Hindustan Aeronautics Limited, New Thippasandra, Bangaluru, Karnataka India

Abstract— Maraging steel belongs to a family of metallic materials with extremely high mechanical strength and good toughness, while agehardenable stainless steels also have good corrosion resistance. The present work involves, evolution of nanostructure C300 grade maraging steel and investigation of heat treatment, mechanical properties and nanostructural development of a new maraging stainless steel. The characterization of the nanostructure was performed by optical microscopy, scanning electron microscope (SEM) and X-ray diffraction (XRD). Mechanical properties were evaluated by Rockwell-C hardness and Charpy impact tests. The heat treatment resulted in an ultimate tensile strength of over 2484 MPa combined with good impact toughness and good resistance against over-aging and relatively good corrosion resistance as well.

Key words: Charpy Impact, Crystallography, Heat Treatment, Martensitic, Toughness and Hardness

I. INTRODUCTION

Numbers of studies have been carried out in the past on the nanostructural aspects of different grades of maraging steels. [4] A majority of these studies had been in the late sixties and the early seventies. After the lapse of nearly a decade interest in this type of steels has recently been revived. As reflected in the series of publications on different maraging alloys of Fe-Ni-Co-Mo and Fe-Ni-Mn types.[9'10] The maraging steel, which is the subject of study in this work, is different from other maraging steels of the types T-300 and C-300 on which a considerable amount of work has been done recently.[14]The important difference between the steel used in this work and the T-300 and C-300 grade steels can be noticed from Table 1, in which the chemical compositions of these steels are given. T-300 is cobalt free, and C-300 contains relatively little titanium. The steel used in the present investigation, on the other hand, contains both cobalt and titanium in a substantial amount.

A high titanium concentration leads to a larger volume fraction of the Ni_3Ti type of phase, and the presence of cobalt makes the formation of the Fe_2Mo type of phase easier. The initial strength of these steels is achieved by the precipitation of a Ni_3(Ti, Mo) type of phase. [18]This is then followed by precipitation of the Fe_2Mo phase which is responsible for the peak strength and also for maintaining high strength on prolonged aging. [8]With this steel being a precipitation hardenable alloy, the dislocation precipitate interaction assumes considerable significance.

Though this aspect has been discussed by some workers, [15] experimental studies to examine it are rather few in other category of maraging steels and non-existent in the category of steel used in the present study. One of the objectives of this work is to ascertain the nature of the dislocation precipitate interaction at different stages of hardening. This task is made difficult by the fact that the volume fraction of precipitates is not very small, and these precipitates are associated with large strain fields. Other objectives of the nanostructural studies are the following: identifying the precipitate phases responsible for strengthening, examining the morphology of precipitates, delineating the sequence of precipitation, and investigating austenite reversion.

II. EXPERIMENTAL METHODS

The material used was vacuum arc melted and vacuum arc re-melted quality C300 grade maraging steel produced by Hindustan aeronautics Limited under laboratory conditions. The material was in the form of forged and machined bars of 50mm diameter and sheets of 5m x 1.5m x 18mm in double solution annealed condition, a process which consisted of heating the material at 910ºC for 2 hours followed by oil cooling and a second annealing at 820ºC for 3.5 hours. The chemical composition of the alloy is given in Table 1.

The cylindrical samples used for dilatometry were 15mm in diameter and 12mm in length machined out from the raw stock with the length of the sample being along the long axis of the bar. A quartz tube dilatometer with manual heating and cooling capabilities was employed. The change in length of the sample was measured using a calibrated dial gage with an accuracy of ±0.0005 mm. The samples were heated to 1473ºC at a heating rate of 10ºC/min, held at that temperature for 60min, and then cooled to room temperature. The cooling rates achieved during the experiments were 25ºC/min up to 400ºC and 10ºC/min up to 200ºC and 4ºC/min thereafter to room temperature. [21]

Chemical composition of maraging steel sample solution			
Element	Wt %	Element	Wt %
Ni	17.5	Al	1.8
Co	6.0	Ag	0.12
Cr	7.2	Mn	2.12
Mo	3.5	C	0.005
Ti	2.3	S	0.03

Table 1: Chemical composition of maraging steel sample solution

Thin foils of grade C300 maraging steel were prepared by window technique and by jet thinning using an electrolyte containing 60% methanol, 34% n-butanol and 6% per-chloric acid to examine transmission electron microscopy (TEM) characters and temperature of the electrolyte was kept below 30ºC.Specially solution treated specimens were ion milled in order to keep the retained austenite. All the thin foils of samples were examined in a JEM-F200 Multi-purpose transmission electron microscope at accelerating voltage of 200kV. Nanostructural Fracture surface of the impact tested samples was conducted in a JSM-7500F Field Emission scanning electron microscope (SEM) to evaluate the failure mode.

Hardness measurements, on a Rockwell C scale, were taken on metallographically polished specimens.

Volume fraction of austenite was estimated from the same samples prepared for metallography. A graphite monochromated Cu Kα radiation was used. The minimum area of sample used was about 20 x 10 mm. The peaks (1 1 0) $_M$ and (1 1 1) $_A$ were selected for analysing the martensite and the austenite phases respectively. [7]

III. Results and Discussion

A. Hardening response of nanostructured C300 steel after aging

Figure 1 shows the hardening response of the material exposed to different temperatures and time periods. The hardness of the solution treated material was 37RC. It could be noticed from Figure 1 that the aging response is so fast that there is no indication of an incubation period for the onset of precipitation. The material showed typical precipitation hardening [1] characteristics in which the maximum hardness was attained on progressively shorter aging as the aging temperature was raised. At 420°C a plateau in the hardness curve was observed after 8hrs of aging, and no softening of the material could be noticed even after 72hrs. At 480°C no discernible softening could be noticed after aging for 24hrs. At 510°C the material attained its peak hardness within 3hrs, whereas at 550°C the maximum hardness was attained in 30min.

The material heat treated to the hardness levels on the ascending portion of the hardness time plot is referred to as under-aged and to the hardness levels on the descending portion as over-aged. It can be seen from Figure 1 that at an aging temperature of 550°C the steel exhibited excellent resistance against overaging for nearly 3hrs. Hardness of 55.38RC was retained even after about 18hrs of aging at this temperature. The results from the isothermal hardness experiments were used for estimating the activation energy for the precipitation reaction. The time (t) taken to attain peak hardness at each aging temperature (T) was used for estimating the activation energy for the precipitation reaction. By plotting the logarithm of the time taken to attain the peak hardness against 1000/T, the results could be fitted into an Arrhenius type of equation,

$$\ln(t) = \frac{Q}{RT} + \text{constant} \qquad (1)$$

Where, Q is the activation energy for the precipitation process, R is the universal gas constant, and T is the temperature of aging in Kelvin. Least square regression was used to fit a straight line to the data points and an excellent fit was obtained. Activation energy of 164±4 kJ/mol was obtained from the slope of the straight line.

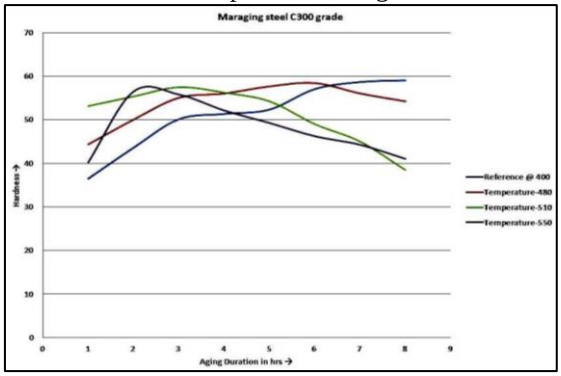

Fig. 1: Effect of aging time and temperature on the hardness of a maraging steel grade C300

B. Mechanical properties of solution treated peak-aged and overaged material

It can be seen that the material after aging at 510°C for 3hrs showed remarkable increase in yield and tensile strength accompanied by a considerable decrease in uniform and total elongation. The load elongation data were analysed in terms of the Ludwik [9, 1] equation.

$$\sigma_t = \sigma_0 + K(\varepsilon_p)n \qquad (2)$$

Where σ_t is the true stress, σ_0 is the stress corresponding to the point of intersection of the elastic and plastic regimes in the stress-strain curve, K is the material constant, and ε_p is the true plastic strain. It's clear that the work hardening exponent of the alloy has substantially reduced after aging. The room temperature impact toughness was reduced from 210J for the un-aged material to 15J after aging for 3hrs at 510°C with continued over-aging, the tensile strength of the material was substantially reduced and the tensile ductility considerably improved. The work-hardening exponent showed progressive increase with overaging. It can also be noticed that prolonged overaging led to the loss of impact energy achieved during the initial stages of overaging.

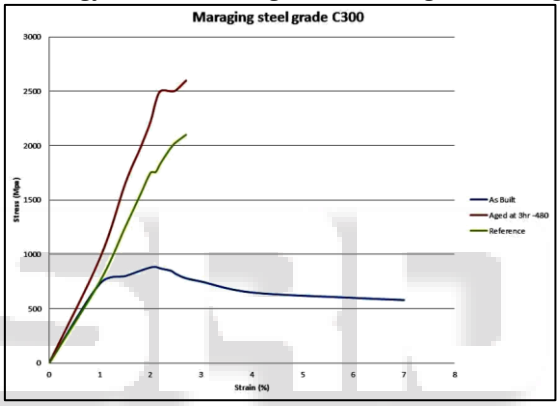

Fig. 2: Typical stress-strain curves for tensile specimens of C300-grade maraging steel tested at room temp.

C. Fractography

Figure 3 shows fracture surfaces of the impact test specimens after cryogenic treatment and aging treatment at 480°C for 3hrs. It is evident that after cryogenic treatment, the fracture surface consisted mainly of fine dimples, which exhibited an entirely trans-granular rupture mode known as micro-void coalescence. Also, there were some large dimples in some regions, in agreement with the high fracture toughness after this treatment. However, the rupture mode of the specimen began to change from ductile to a brittle appearance when aged at 480°C. It can be seen that failure had occurred via a mixed mode of ductile and cleavage-like fracture.

D. Nanostructural Studies

1) Nanostructure of solution-treated under-aged and peak aged material

Substructure of the martensite phase was made up of a high density of dislocations. No evidence of nano-twins within the laths could be seen in the regions examined. Specimens aged at 510°C for 30min were examined to study the early stages of precipitation. Figure 3 shows the nanostructure of such a specimen. The lath morphology was very similar to that seen in the solution treated specimen. Prior austenite grain boundaries could be seen in certain regions.

Thin foils of specimens aged at 510°C for 3hrs showed predominantly the presence of a martensite phase. Precipitate size on average was found to be about 60nm in length and about 8nm in thickness. The precipitates though quite small were found to show a variety of fringe contrast which could be seen clearly in the dark field images obtained by using precipitate reflections. The patterns from the precipitates in the specimens aged for 30min and 3hrs at 510°C could be indexed in terms of the hexagonal Ni_3Ti type, eta (η) phase having lattice parameters a = 0.7804nm and c = 0.9725nm. Since this phase has been found to contain Mo which lead to form Ni_3 (Ti, Mo) phase. In addition to the rod-shaped precipitates the specimens aged at 510°C for 3hrs showed the presence of nearly spherical precipitates and diffraction patterns from these particles could be indexed in terms of the hexagonal Fe_2Mo phase.

E. Nanostructure of overaged material

For characterizing the nanostructure of the overaged steel, two extreme aging temperatures, namely, 480°C and 510°C were selected.

1) Specimen overaged at 480°C for 8 hours

Thin foils of specimens subjected to this heat treatment showed martensite as the predominant phase. The martensite substructure in these specimens was not much different from that obtained from the specimens aged at 550°C for 3hrs. Initially it contained a substantial quantity of austenite while the latter was free of austenite. Austenite phase was present mostly between the martensite laths and could be placed in the category of inter-lath austenite. The pattern taken from the regions containing martensite and austenite phases showed that the two lattices obeyed the Nishiyama Wassermann orientation relationship, which can be stated as (110) bcc // (111) fcc and [100] bcc // [110] fcc.

Along with the lath austenite we could also see recrystallized austenite in the material. This morphological form of the austenite was also found to obey the Nishiyama Wassermann orientation relationship. As in the case of the specimens aged at 550°C for 3hrs. Specimens aged at 480°C for 8hrs also showed a homogeneous distribution of second phase particles of Ni_3 (Ti, Mo) type phase.

Average precipitate size was found to be nearly 316nm in length and 60nm in width. Dark-field microscopies of some precipitates were indicated that with the segments arranged in a direction perpendicular to the length of the precipitate. This appearance was suggestive of internal twinning of the precipitate particles and these precipitates were of the Fe_2Mo phase.

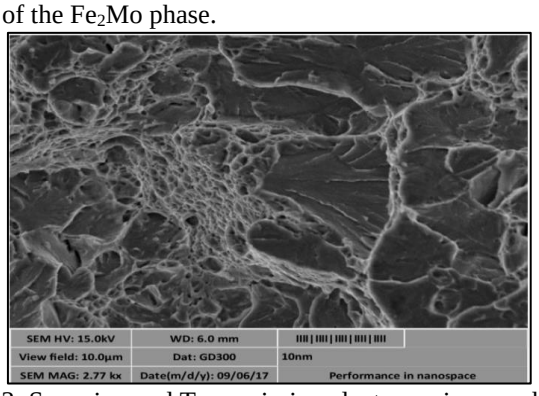

Fig. 3: Scanning and Transmission electron micrographs of the designed steel (grade C300) after oil cooling at temperature 480^0C.

2) Specimens overaged at 510°C

The SEM investigations were carried out on samples subjected to overaging at 510°C for 3hrs and 8hrs. In the specimen overaged for 3hrs, the basic nanostructure comprised of parallel arrangement of laths of the martensite phase. The appearance of the laths was more or less similar to the martensitic structure observed in the solution treated sample .The main difference being the presence of a second phase at the lath boundaries. The relationship between the austenite and the martensite phases in the specimens overaged for 8hrs at 510°C was found to be [110] bcc // [111] fcc and [111] bcc // [110] fcc and the matrix phase was found to be lath martensite. [17]

3) Nanostructure after Deformation

Nanostructures of the alloy aged at 480°C for 3hrs and at 510°C for 8hrs were examined after deforming until fracture, in order to ascertain the nature of the dislocation precipitate interaction. The nanostructure of the alloy aged at 480°C for 3hrs and deformed consisted of lath martensite [11]. Due to the high-dislocation density, it was not possible to image the dislocation structure very clearly. Extensive dark-field electron microscopy was carried out to examine the effect of deformation on the precipitates.

IV. CONCLUSIONS

The following conclusions could be drawn from the experiments:

1) The strengthening precipitates in C300 grade maraging steel are the Ni_3Ti, Ni_3Mo and Fe_2Mo inter-metallic phases. The Ni_3Ti, Ni_3Mo type of phase forms by heterogeneous nucleation on the dislocations.
2) In the peak-aged condition, the deformation of the material is associated with the shearing of precipitates by dislocations. The material in this condition exhibits an extremely low work hardening.
3) Cobalt leads to formation of Fe_2Mo which adds material to its high strength at peak stage and remain even after ageing.
4) Grain size is greater due to the presence of high % Al in maraging steel.
5) Ti and Mo will form inter metallic phases like Ni_3Ti, Ni_3Mo and Fe_2Mo at 480^0C.
6) Fe and Co are responsible to form nano size grains of Ni_3Mo when oil treated at 550^0C ageing temperature and annealed at 900^0C.
7) Ni_3 Mo will cause to form precipitate of Fe Ti and this will give higher proof stress in the material to decide type of grade of the material

REFERENCES

[1] Decker.R.F., et al., Proc. Symp. Relation between the Structure and Properties of Metals, NPL, Teddington, England, 1963, pp. 648-71.
[2] Dieter.G, et al. Mechanical Metallurgy, McGraw-Hill, vol.10, 1986, pp.15, 123-154,248.
[3] Degarmo.E, et al. (2003), Materials and Processes in Manufacturing (9th ed.), Wiley, p. 119, ISBN 0-471-65653-4
[4] Floreen.S, et al. Metal composites and mechanical properties, 1968, vol. 13, pp. 115-28.

[5] Lecompte.J.B, et al. Material Science 1985, vol. 20, pp. 3339-52.
[6] Ludwick.P, et al. Elemente Der Technologischen Mechanik, Springer Verlag, Berlin, 1909, p. 32-48.
[7] Kudjumov.G, et al. Z. Phys., 1930, vol. 64, p. 310-325.
[8] Krishtal.M.K., et al., in Diffusion Processes in Iron Alloys, Translated from Russian by the Israel Programme for Scientific Translations,vol.25,1998
[9] Nicholson, et al., Strengthening Methods in Crystals, Elsevier Publishing Co., Amsterdam, 1971, pp. 261-325.
[10] Nishiyama.Z, et al. Sci. Rep. Tokohu Univ., 1934, vol. 23, p. 560-638.
[11] Perkas.M.D, et al., Met. Sci. Heat Treat, 1968, vol. 6, pp. 415-425.
[12] Peters.D.T, et al., Trans. A1ME, 1969, vol. 245, pp. 2021-26.
[13] Wayman.M, et al., Acta Metall., 1966, vol. 14, pp. 347-69.
[14] Ronald A,et al. Engineering Fracture Mechanics, Volume 25, Issue 4, 1986,pp.435-478,483,486
[15] Rack H.J.,et al. Metallurgy, 1971, vol. 2, pp. 2306-08.
[16] Sinha.S.S et al. Maraging steels data book ,HAL-Industrial Publications,pp.56,83-97,253-270,291-315, 351-378, 381,389,412-432.volume 4,1986
[17] Shiang.L., et al., Metallography, 1988, vol. 21, pp. 425-50.
[18] Singh.J, et al. Mater. Sci. Eng., 1987, vol. 94, pp. 233-42.
[19] Sass.S.L, et al., Trans. AIME, 1969, vol. 245, pp. 1836-38.
[20] Tuffnell.G.W,et al ASM, 1968, vol. 61, pp. 798-806.
[21] Villars.P, et al., Pearson's Handbook of Crystallographic Data for intermetallic Phases, ASM, Metals Park, OH, 1985, vol. 3, p. 2905-2954.
[22] Vanderwalker. D.M., et al. Metall. Trans. A, 1987, vol. 18A, pp. 1191-94.
[23] Vasudevan.V.K. et al. Metall.Trans.C, vol. 21A, 1990, pp. 2655-68.
[24] Wayman.C.M.,et al. Metallography, 1988, vol. 21, pp. 399-423.
[25] Wassermann.G, et al. Arch. Eisenhiitt, 1993, vol. 16, p.365, 582, 647.

